APPLICATION OF CFD TOWARDS THE THERMO-HYDRAULIC ANALYSIS OF SPENT FUEL POOL ACCIDENTS

R. Oertel, E. Krepper, D. Lucas
Helmholtz-Zentrum Dresden-Rossendorf e.V.
Postfach 510119, 01314 Dresden
r.oertel@hzdr.de, e.krepper@hzdr.de, d.lucas@hzdr.de

ABSTRACT

The thermo-hydraulic analysis of Spent Fuel Pool accident scenarios is predominantly carried out using one-dimensional codes. This implies that simplified assumptions have to be made for the flow paths around the storage racks and inside the reactor building. Here, CFD is employed to investigate the convective phenomena involved and to examine their relevance for the cooling of the individual fuel assemblies, which themselves are modeled as porous bodies. The paper includes a discussion of relevant thermohydraulic aspects and the modeling on the fuel assembly scale as well as the reactor building scale. First preliminary large scale simulations are presented, using the design of Fukushima's Unit 4 with the corresponding Spent Fuel Pool loading as a test case. A loss of coolant due to the outage of the cooling system and subsequent boil-off is assumed, leading to partially or fully uncovered fuel assemblies. The emerging flow paths are described qualitatively. This ongoing work gives an outlook how CFD can help to study the safety of Spent Fuel Pools as a standalone tool or by delivering input to one-dimensional codes.

KEYWORDS
Spent Fuel Pool Safety, Boil-Off/Drainage Scenarios, CFD, Porous-Body-Approach

1. INTRODUCTION

Typically for the first five to ten years after a fuel assembly is removed from the reactor core, its decay heat is still too large for pure conductive cooling. It is placed in a Spent Fuel Pool (SFP) and cooled by natural convection flow in the water phase. The pool cooling system keeps the contained water at approx. 25°C. Although the decay heat per fuel assembly is only of the order of kilowatts (≈ 0.2-20kW for a BWR-type fuel assembly), the generally large inventory of several reactor cores can result in a total heat production in the SFP of the order of megawatts. Two scenarios, namely (1) the outage of the cooling system followed by boil-off or (2) the loss of coolant due to leakage along the wall, might lead to a dewatering of the pool. The accident in Fukushima was accompanied by the loss of external and emergency power supplies and is an example for the former scenario. According to Kaliatka et al. [1], the water level in the SFP of Unit 4 decreased more than 6.5m, down to 1.5m above the top of the fuel assemblies. Concerning the loss of coolant scenario, Ibarra et al. [2] have reviewed 12 years of U.S. NPP operating experience. They report several incidents of accidental partial drainage, two of them exceeding 1.5m. The corresponding initiation mechanisms are not further discussed here.

The stored fuel assemblies are usually arranged in high-density racks as shown in Fig. 1. The radial boundary condition for a centrally stored fuel assembly is almost adiabatic and cross-flows are not possible. The dominant cooling path lies along the axial direction. If the water-level decreases below the top of the fuel racks, the regular circulation paths in the water phase are blocked. As soon as the water

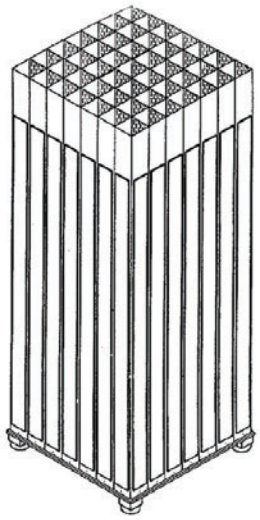

Figure 1. High-Density Fuel Rack. [3]

level reaches the heated length, the fuel rods will heat up beyond the water temperature. At a certain water level, the remaining cooling mechanisms are unlikely to keep the temperatures in the uncovered section low enough to prevent an exothermic oxidation of the zirconium cladding, followed by the release of fission products. For the case of dewatering by evaporation, the dominant heat transfer mechanism is forced convection due to the steam produced at the water surface. For the case of dewatering by leakage, the water might not reach saturation conditions at all. Then, the axial heat conduction along the fuel rods towards the head of the fuel assembly as well as into the remaining water is an important cooling mechanism. Especially for the latter case, the boundary conditions at the top of the fuel assemblies, i.e. the flow phenomena above and around the racks, determine the evolving peak temperatures.

For nuclear safety assessments one-dimensional system- or integral codes are used in most cases. Benjamin et al. [4] developed SFUEL to calculate the temperature development in a drained SFP for a range of parameters like storage rack design, building ventilation, fuel burnup and others. While assuming an instant and complete loss of coolant, they note that this is not the most conservative assumption regarding the accident path, since partial drainage blocks the path for natural convection of air and is therefore more severe. Nourbakhsh et al. [5] addressed some of the drawbacks of SFUEL and developed SHARP, which was also used for sensitivity calculations, provided the pool is completely drained. More recently, Kaliatka et al. [1,6] have applied ATHLET-CD, ASTEC and RELAP5 to examine the safety of the SFP's at the Ignalina NPP in Lithuania, which was shut down for decommissioning in 2009. Both, the outage of cooling systems and the loss of coolant due to leakage were taken into account. At the Ignalina NPP, two channel-type boiling water reactors have been in operation, each of them equipped with a system of spent fuel pools. Kaliatka et al. modeled them as a single pool, neglecting the influence of global convection paths entirely. In the aftermath of the Fukushima Accident, the Sandia National Laboratories issued an Accident Study [7], which includes results and a discussion of TRACE and MELCOR calculations for the SFP of Unit 4 that emphasizes the importance of the building air exchange with the outside environment.

In general, the former codes are designed for the thermo-hydraulic analysis in constrained channels, where mostly unidirectional forced convection is present. Although fast and suitable for captioning transient phenomena in large scale systems, these codes are not entirely qualifyed for calculations concerning SFP-related accident scenarios for the following reasons: Three-dimensional effects like the mixed convection flow in the reactor building and the pool region above the storage racks need to be

modeled in an averaged sense, using correlations for heat and mass transfer. The effects of air-steam mixing, thermal stratification and natural convection as well as their feedback on the local temperature development are insufficiently represented. Simplified assumptions have to be made for the flow paths above and around the racks, although it is not clear whether they occur under all circumstances. Moreover, the prediction of natural convection flow rates depends on the knowledge of the three-dimensional temperature distribution and fluid composition. This makes the application of CFD appear a promising alternative.

Using the FLUENT CFD-Code, Boyd [3] predicted flow patterns and peak temperatures, assuming a complete and instant loss of coolant. The computational domain included half of the reactor building and the SFP, utilizing a symmetry boundary condition. The fuel racks were treated as a contiguous porous body. Boyd conducted similar sensitivity studies like Benjamin et al. [4]. Indicating the predictions as best estimates, he determined peak cladding temperatures in the range of 600 to 800°C after a minimum decay time of two years, while the hottest fuel (BWR) still produced roughly 1kW of decay heat. To the knowledge of the authors, no comparable studies have been conducted that include the entire reactor building in the computational domain. In the literature, no CFD-studies concerned with partially uncovered fuel assemblies in a pool atmosphere could be found. Yet, it can be thought of as a rather severe scenario, given the fact that the natural circulation path through the assemblies is blocked in the case of high-density racking.

The present paper presents ongoing work. It discusses the thermohydraulic phenomena on the fuel assembly scale and the porous-body modelling with the according heat transfer and pressure drop characteristics. First large-scale simulations that include an entire fuel pool and the respective reactor building atmosphere are presented and discussed qualitatively. Each fuel assembly is treated as a separate domain with appropriate boundary (transition) conditions. Partial as well as a complete loss of coolant due to boil-off are postulated. It is shown that this approach allows systematic studies of temperature distributions for a great variety of parameters. Among those, one of the less researched aspects is the spatial arrangement of the fuel racks in the pool, their spacing and other geometric characteristics and their impact on the cooling of the single fuel assembly.

2. FUEL ASSEMBLY SCALE

2.1. Thermohydraulic Aspects

As outlined in section 1, two accident scenarios are conceivable: Either a failure of the pool cooling system or leakage somewhere along the SFP-wall. In the absence of mitigating measures, the water level will reach the heated length, leading to gradually rising cladding temperatures in the uncovered section. At this point, the heat up rate can be estimated by

$$\frac{\Delta T}{t} = \frac{\int_{z_{waterlevel}}^{z_{top}} \dot{Q}'(l)\, dl}{m'_{FA}\, l\, c_{p,FA}(T)} \tag{1}$$

where $\dot{Q}'$ is the decay heat power per unit length as a function of the uncovered length l and m'_{FA} the mass of the fuel assembly per unit length. This relation is valid providing that no steam is produced, no heat is transferred into the water and the boundary conditions of the fuel assembly are fully adiabatic in all other directions. If $\dot{Q}'(l)$ is a constant, the heat up rate is independent of the water level and the loss rate. The question arises to which extend the remaining passive cooling mechanisms slow down the heat up rate and at which peak temperature they are in balance with the decay heat production. These mechanisms are illustrated in Fig. 2 for the partially drained SFP and will be discussed in the following section.

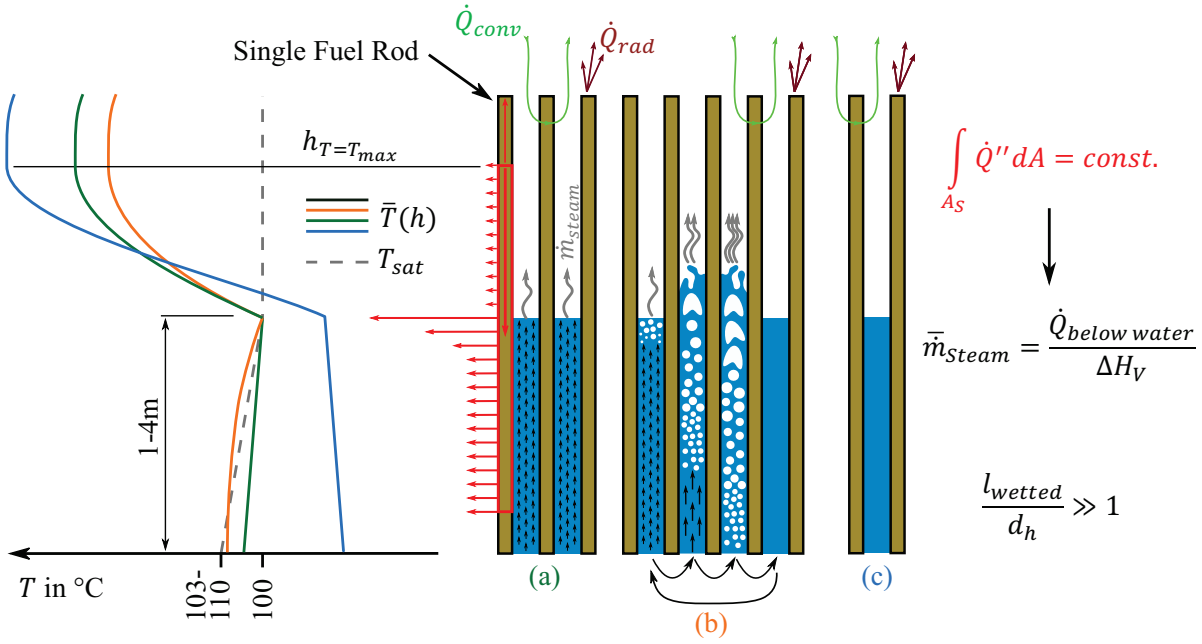

Figure 2. Thermohydraulic Aspects for the partially drained SFP.

Scenario (a) takes place when the water has reached saturation temperature. Steam is produced at the interface and superheats as it rises inside the fuel assembly. The amount of heat that the steam carries away determines the peak temperature. The steam mass flow is given by the heat released in the water phase. The simple fact that becomes apparent here is: In the absence of other cooling mechanisms than forced convection due to steam production, the peak temperature only dependents on the ratio of the heat released above and below water. Therefore the axial power profile is crucial and the total decay heat power plays a rather negligible role. This is particularly valid for the centrally stored fuel assembly. What has to be taken into account here is the axial temperature gradient along the fuel rods in the gas phase. A part of the released heat in the uncovered section is conducted into the water phase where it contributes to the steam production. The maximum cladding temperatures are reached at the end of the heated length. Above that, the temperature remains at a constant value or declines slightly, depending on the boundary conditions at the upper end. Because the decay heat production is a constant for the timescales of the fluid flow, the steam mass flow rate can be calculated via the quotient between heat released below water and the latent heat of evaporation. This allows treating the problem in a single phase manner, by considering the water surface as a no slip wall with a temperature of 100°C. The steam mass flux is included as a boundary source, depending on the heat flux due to axial conduction and the heat released in the water phase. What has to be kept in mind is that this gives only the time-averaged steam mass flux. At this point a closer look at the boiling behaviour is necessary. A total decay heat production between 100W and 20kW for a single BWR-fuel assembly corresponds to a heat flux at the cladding surface of the order of 10^2-10^3W/m². From the Nukiyama-curve (see Fig. 3) for pool boiling it is evident that convective boiling can be expected. The phase change takes place at the water surface and all the heat from below is transported there through natural convection. The heat flux is generally not high enough to sustain steady nucleate boiling. Here, the difference in comparison to pool boiling is that the volume available for flow in the fuel assembly is divided into sub-channels. They have a high length to diameter ratio and exhibit a higher flow resistance in the radial then in the axial direction. Additionally, the heat source is uniformly distributed over the volume which results in small temperature differences. Little or no fluid circulation occurs and an imbalance between the heat production below water and the heat transport rate towards the

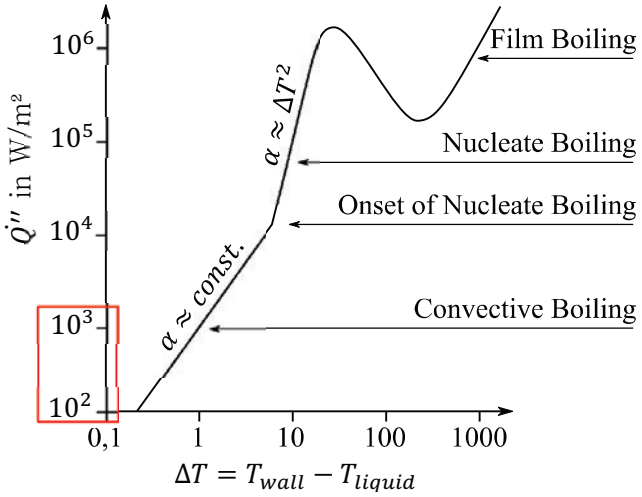

Figure 3. Nukiyama Curve for Pool Boiling under atmospheric Conditions.

phase interface develops. Schulz et al. [8, 9] conducted experiments on the boil-off scenario that indicate that this imbalance causes an instability in the boiling regime. They have provided the raw data from their experiments, which is further processed and interpreted in the present work. The experimental setup is sketched in Fig. 4.

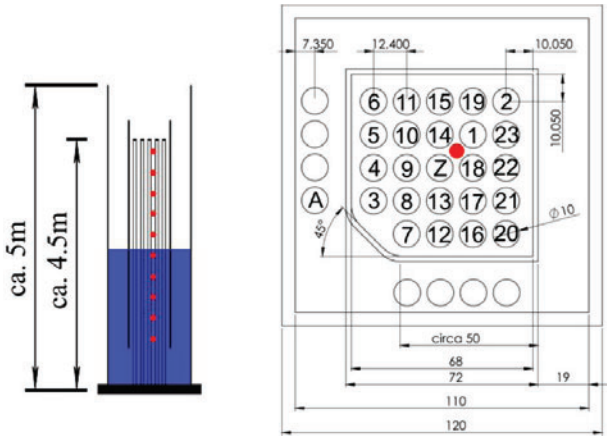

Figure 4. ADELA II Experimental Facility and Thermocouple Locations for the present Discussion. [8]

The inner channel represents one quarter of a typical BWR-fuel assembly, using electrically heated rods. The outer and the inner channel are hydrodynamically coupled at the bottom. The equally heated auxiliary rods are meant to establish near- adiabatic boundary conditions, simulating the situation for a centrally stored fuel assembly in a fuel rack. Here, the focus lies on the temperature distribution along the axial direction in the center of the cross section. Schulz et al. [9] report that the change in the boiling regime during the boil-off process is audible. Although the ADELA II facility did not allow any visual access, the temperature development at several axial locations, in conjunction with the water level, delivers a conclusive explanation of the process. Schulz et al. have provided the raw data from their experiments for further processing in this work. As displayed in Fig. 5 for less than 40 hours of test duration, the

temperature increases continuously as soon as the respective location is exposed to the steam atmosphere. Apparently, the actual steam mass flow rate equals its time average. The change in the boiling regime occurs for the timespan between 40 and 53h and a water level between 1.5 and 2.5m.

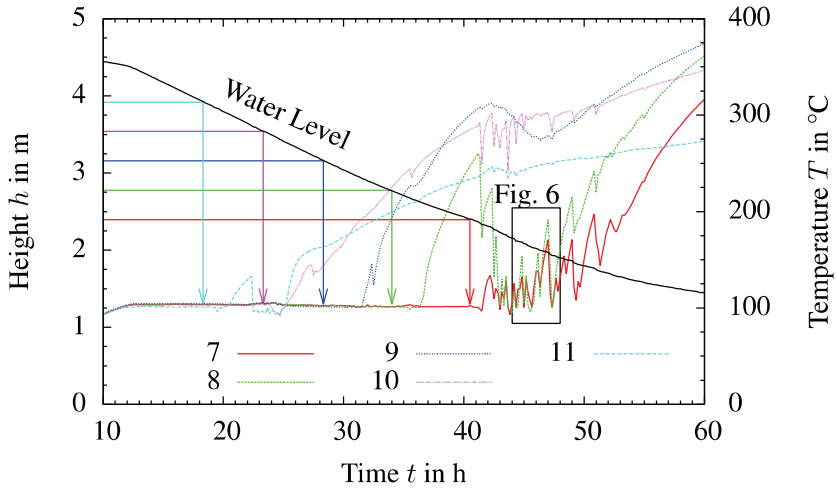

Figure 5. Development of the Water Level and Fluid Temperature at different Locations for 20W per Rod.

The phenomenon is plotted again in Fig. 6 with a finer temporal resolution. For the given heat input of 20W per rod (≈ 2kW for the assembly), the fluctuations are subject to a frequency of approximately four outbursts per hour. For a higher decay heat similar effects occur, but with a higher frequency.

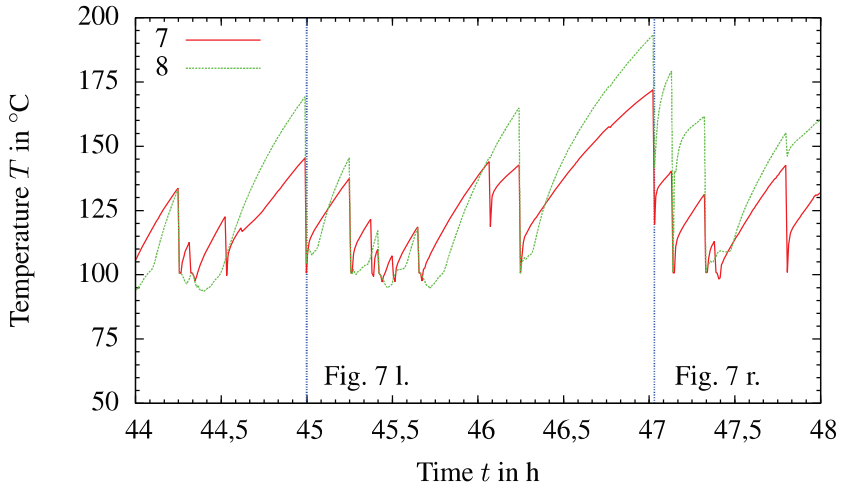

Figure 6. Development of the Fluid Temperature for 20W per Rod.

The axial temperature profile below water allows a better understanding of the process. The data plotted in Fig. 7 corresponds to the two points in time highlighted in Fig. 6. In Fig. 2, the sequence of events is illustrated, labelled as scenario (b). At first, as previously described, an imbalance between the heat production below water and the transport rate towards the interface develops. Because of the hydrostatic

pressure gradient, the saturation temperature increases linearly at about 2.4K per meter water depth. Therefore the water temperature below the interface reaches values well above 100°C as evident from Fig. 7 for both points in time at -480s. A change in the hydrostatic pressure will then result in abruptly superheated water and subsequent rapid boiling. The initiating event can be a single bubble rising and expending on its way up or sudden nucleate boiling near the interface, occurring due to the increased heat flux as a consequence of the axial heat conduction along the fuel rods.

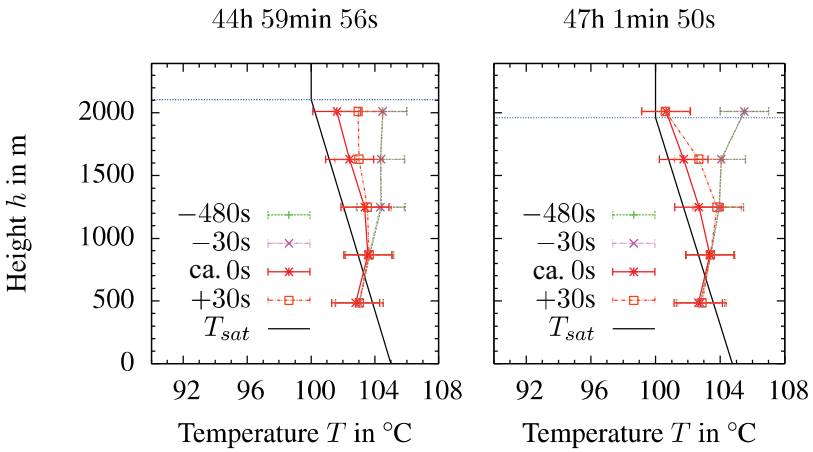

Figure 7. Axial Temperature Profile for selected Times Spans.

Either way the rapid boiling leads to a temperature decrease in the water phase (see “ca. 0s” in Fig. 7.). The fluid expulsion goes along with quenching at elevated locations (see Fig. 6). Immediately after the event, it can be expected that the steam production is considerably less than the average. It takes some time until the temperatures below water reach their peak values again (see for example +30s in Fig. 7). The absence of the steam production goes along with less cooling of the rods in the gas phase. The heat up rate converges to values gained by equation (1). Whether the deficiency of the steam production will lead to peak temperatures in the gas phase that are considerably higher than those calculated on the basis of the average steam mass flow assumption is uncertain. Yet it is crucial to keep in mind, that using the average (i.e. a constant) steam mass flux is not an appropriate assumption under all circumstances. Yet it serves well for basic investigation.

Scenario (c) in Fig. 2 describes the situation for a loss of coolant due to leakage. The water did not have enough time to reach saturation temperature and the steam production will not serve as a cooling mechanism for the uncovered section. The uniform heat up in the gas phase suppresses fluid circulation through the entire fuel assembly. It is now the flow situation around the fuel racks that has the largest influence on the peak temperature in the core of the single fuel assembly. The heat transport in the assembly happens mainly by means of heat conduction.

2.2. Balance Equations and Modelling

The prior discussion of the thermohydraulics inside the fuel assemblies allows the formulation of the balance equations for the fuel assemblies, in conjunction with an appropriate degree of modelling. The fuel assemblies are treated as porous bodies. This implies that geometric details are neglected in the course of the spatial discretization. No distinction is made between fuel rods and sub channels. The fields for velocity and temperature are calculated in an averaged sense. As a result of the averaging procedure, supplementary relations are required to incorporate the appropriate pressure loss and heat transfer

characteristics of the flow inside the fuel assembly. The CFD-Code ANSYS CFX is adopted here. The governing equations for laminar single-phase flow in porous media read:

$$\frac{\partial}{\partial t}(\gamma\rho_f) + \nabla\cdot(\rho K\cdot\vec{u}) = 0 \tag{2}$$

$$\frac{\partial}{\partial t}\left(\gamma\rho_f\vec{u}\right) + \nabla\cdot\left(\rho_f(K\cdot\vec{u})\otimes\vec{u}\right) = -\gamma\nabla p_f + \nabla\cdot\left(\mu K\cdot(\nabla\vec{u} + (\nabla\vec{u})^T) + \frac{2}{3}\delta\nabla\cdot\vec{u}\right) - \gamma\frac{f}{d_h}\left(\frac{\rho_l}{2}\vec{u}^2\right) + \gamma\rho_f g \tag{3}$$

$$\frac{\partial}{\partial t}\left(\gamma\rho_f h_f\right) + \nabla\cdot\left(\rho_f K\cdot\vec{u}h_f\right) = \nabla\cdot\left(\lambda_f K\cdot\nabla T_f\right) + \alpha A_{fs}\left(T_s - T_f\right) \tag{4}$$

$$\frac{\partial}{\partial t}(\gamma_s\rho_s c_s T_s) - \nabla\cdot(\lambda_s K_s\cdot\nabla T_s) = -\alpha A_{fs}\left(T_s - T_f\right) + \dot{Q}_s''' \tag{5}$$

Each computational control volume in the fuel assembly domain consists of a fixed fluid and solid fraction. The volume porosity $\gamma = V_{flow}/V_{total}$ describes the portion of each control volume that is available to the flow, $\gamma_s = \gamma - 1$ being the solid volume fraction. Correspondingly, the area porosity $K = A_{flow}/A_{total}$ describes the portion of each control volume face available for the flow, relevant for all convective/diffusive terms. It is anisotropic for a rod bundle configuration. The viscous and inertial losses due to flow along the rods and past components such as spacers and tie plates are accounted for using a loss term (3rd on RHS) in the momentum equation (3). Accordingly, the heat transferred between the heat releasing rods ($\dot{Q}_s'''$ in Eqn. (5)) and the fluid is modelled as a source term (2nd on RHS) in the energy equation of the fluid (4) and a sink term (1st on RHS) in the energy equation for the solid (5). The latter equation is necessary to describe the heat conduction in the solid part, which is an additional cooling mechanism for the case of partially uncovered fuel assemblies (see section 2.1). Herein, the heat conductivity λ_s is also anisotropic, being zero in the crosswise and of finite magnitude in the lengthwise direction of the fuel assembly. All solid material properties used here are mass weighted averages, including the contributions of the cladding and the fuel. The modelling terms include geometry dependent parameters, such as the hydraulic diameter $d_h = 4A/U$, calculated from the cross-sectional area available to the flow and the wetted circumference. A_{fs} represents the interfacial are density between the solid and the fluid as the wetted surface area per unit volume. The two remaining quantities needed to close the system of equations are the friction factor f and the heat transfer coefficient α. Their determination requires knowledge about the flow regime. From the experiments of Schulz et al. [8, 9] it is known that the Reynolds number $Re = \rho d_h v/\mu$ lies well below $Re = 100$ for the boil-off scenario. Similar results can be obtained using the formula for the steam mass flow in Fig. 2. As evident from Fig. 8, this Reynolds number range corresponds to laminar flow for a wide range of pitch to diameter ratios between the fuel rods. The flow inside the sub channels stays laminar up to Reynolds numbers of at least 200. For laminar flow, the friction factor is a linear function of the Reynolds number and can be obtained theoretically. The overall friction factor of a fuel assembly consists of several contributions. The largest contribution comes from the viscous loss due to the flow inside the sub channels, which themselves are differentiated into central, corner and wall sub channels. Here, the friction factor relations from Kakaç et al. [10] for fully developed flow are used. The contributions of the different sub channel types are weighted according to the flow area they take up. For the momentum loss across spacer grids no relation of general validity is available. Two fin type spacer grids were compared concerning the pressure loss they cause. For the given flow parameters, no difference could be detected between them. The rise in the pressure loss was almost a linear function of the Reynolds number and about five times higher than for the empty sub channel. Knowing the number of spacer grids per fuel assembly, an effective contribution

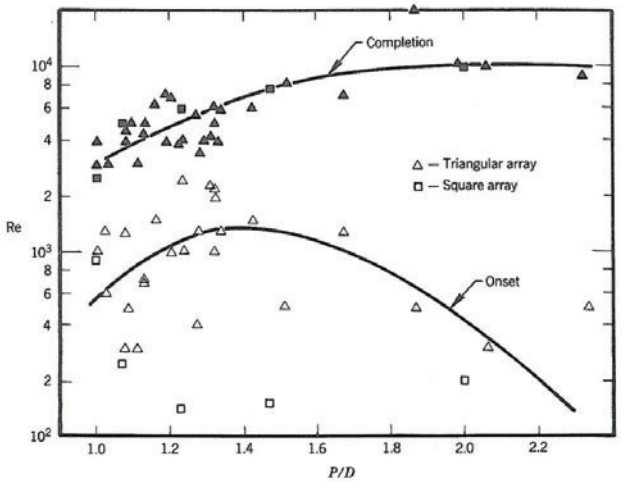

Figure 8. Onset of Turbulence. [10]

to the friction factor can be calculated. Concerning the entrance effects on the base plate hole and the loss across the lower and upper tie plates, the relations from Nourbaskhsh et al. [5] were used. The heat transfer characteristics inside a sub channel can be expressed in terms of the Nusselt number $Nu = \alpha d_h/\lambda$. It is a constant for laminar flow conditions. Kakaç et al. [10] give values for a series of sub channel types for developing and developed flow as well as different P/D ratios and boundary conditions. For the given flow situation, i.e. small velocities and a large heat transferring area, the experiments of Schulz et al. [8, 9] showed that the difference between the cladding and the fluid temperature is generally of the order or 1K. A differentiation between corner, wall and central sub channels concerning the heat transfer is therefore not necessary. The present calculations are based on the values given by Kakaç et al. [10] for the central sub channel. The relations for the pressure loss and heat transfer utilized here have been verified via geometry-resolved calculations of a central sub channel and were found to be valid.

3. POOL AND REACTOR BUILDING SCALE

3.1. Thermohydraulic Aspects

The flow characteristics above and around the fuel racks and in the reactor building are quite different from the flow inside the assemblies. Because of the large length scales involved, the flow paths are subject to spatial and temporal fluctuations. While the flow inside the assemblies is mostly laminar, the flow above the racks and inside the reactor building is expected to be turbulent, mainly induced by buoyancy effects. The situation compares well to common HVAC-cases (Heating, Ventilation and Air Conditioning Simulations), with ventilation into and out of the reactor building, the water surface as an additional mass source and the uncovered portion of the fuel assemblies as a heat source. What is uncommon to usual HVAC simulations are the great temperature differences involved, of the order of several 100K. Use of the Boussinesq-Approximation and otherwise constant material properties is not permissible here. It is essential to use a variable density (real gas properties) and to incorporate the temperature dependence of the thermal conductivity and specific heat capacity. E.g. when determining how wide a down comer region between two vertically arranged heated structures (fuel racks) needs to be, in order for the cooler air to reach the pool floor, the exact knowledge of the thermal conductivity is important. For air it rises significantly with the temperature and has an equalizing effect on the temperature profile in the flow region. The temperature difference which drives the flow might be diminished, resulting in even higher temperatures. If the thermal conductivity is underdetermined, the flow rates will be overdetermined for this particular case. Another important aspect that needs to be

considered is the mixing of air and steam above the fuel racks. The steam rises from the fuel assemblies in the form of a plume, formed and accelerated by surrounding air vortices. This determines the rate at which heat is transported from the pool towards the building atmosphere. In turn, this necessitates a careful consideration of the resulting properties of the mixture, depending on the respective mass fractions of air and steam.

3.2. Modelling

The balance equations solved on the building scale equal the equations (2)-(4), excluding the modelling terms for heat transfer between fluid and solid as well as the momentum loss. Additionally, the k-ω based Shear-Stress-Transport model is used to predict the eddy viscosity. In the k-Equation, a term modelling the turbulence production due to buoyancy is incorporated. As discussed in section 2.1, the system boundary is drawn along the water surface and considered to be a no slip wall with a temperature of 100°C. Steam is introduced into the domain at all fuel assembly locations, based on the released heat below water (see Fig. 2). In relation to the time scales of fluid flow, the water level is assumed to be constant. Every fuel assembly is treated as a separate domain with a free slip boundary condition along the channel wall. The momentum loss in the assemblies is entirely modelled as described in section 2.2. This allows the use of a coarse computational grid with hexahedral cells with a width of 3.5cm. The same value is applied to the regions above and around the racks. Starting from above the racks, the grid resolution is chosen gradually coarser, up to a cell width of 0.2m for the reactor building atmosphere. Heat transfer between the assemblies is permitted and the domain interfaces are modelled as thin steel walls. The fuel rack walls on the side of the pool atmosphere are subject to a no slip boundary condition. Concerning the material properties, the IAPWS formulation is used for steam and real gas properties are used for air. The mixing between air and steam is assumed to be ideal. The respective mass fractions are obtained by solving an additional transport equation for one component while both share the same velocity field.

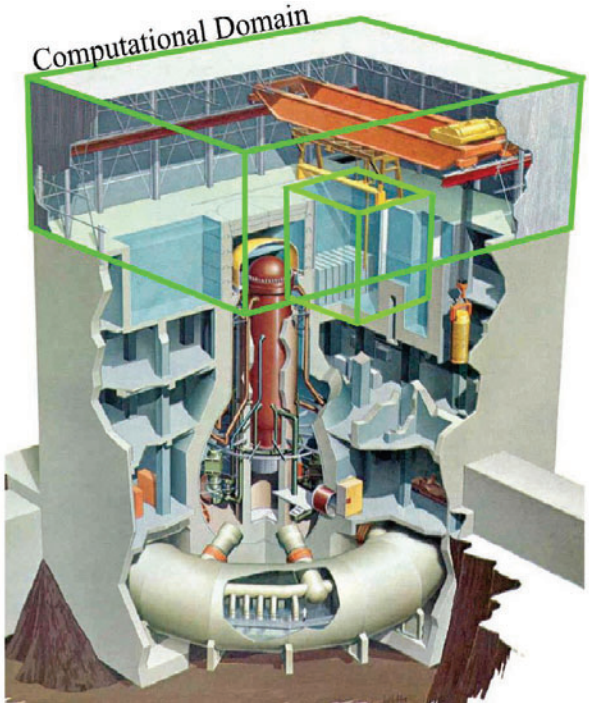

Figure 9. Mark I Reactor Containment Design and Computational Domain for the Test Case.

3.3. Test Case

The design of Fukushima's Unit 4 is used here as a test case, because information about the spent fuel pool loading (incl. locations of the fuel) as well as the rack design and the fuel assembly type is available in the literature [7]. The reactor was in refueling mode before the accident. Fuel assemblies with a short decay time period resided in the pool. The hottest fuel assemblies produced about 3.5kw during the time of the accident. Fig. 9 shows the computational domain for the present calculations. All boundaries represent adiabatic no slip walls, except for the roof which was specified as a combined inlet and outlet boundary condition. Depending on the internal velocity field, fluid is allowed to leave the domain and air at ambient conditions (25°C) can enter. The building was assumed to be free of rubble or machinery. Because of the different time scales between heat production in the solid and the fluid flow, the simulations were first run towards a steady state in terms of global averages for temperature and velocity, using a solid time step several orders larger than for the fluid. The results for two scenarios are presented in the following section. A steady state in a residual sense cannot be achieved this way, because the flow due to natural convection is subject to time dependent fluctuations. Using the steady state results as an initial guess, further transient simulations need to be conducted, using equal values for the fluid and solid time step. This way, the fluctuations in the convective paths can be quantified.

4. PRELIMINARY RESULTS

Fig. 10 shows the streamlines starting from the water surface inside the fuel assemblies together with the respective temperature. The water level in this example case is 2.8m above the pool floor. This

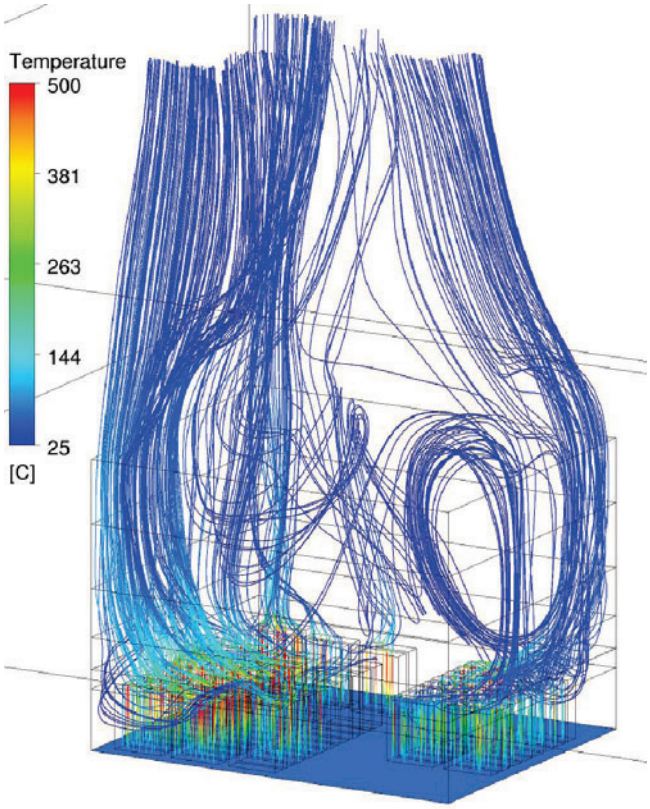

Figure 10. Streamlines and Temperature Distribution in the Pool for a Water Level of 2.8m (1.7m below top of the Fuel Racks).

corresponds to an exposed length of 1.7m. The rising steam superheats up to a maximum temperature of approx. 500°C. Similar temperature ranges for this water level are reported in [7] and were obtained using TRACE. The rising steam plumes tend towards the walls on either side of the pool, while mixing with ambient air entering the pool atmosphere. They reach an average terminal velocity of about 3 to 4m/s just 2m above the top of the racks, becoming narrow as a result. The fuel assemblies located in the middle of the pool are subject to air overflow, which dictates the boundary condition at their upper end and therefore the internal peak temperature. An interesting question arising here is how the location of the hottest fuel influences the flow paths and therefore the overall cooling performance of air entering the pool. Another scenario that the presented approach was tested on is a complete loss of coolant. For the pool loading of Fukushima's Unit 4 at the time of the accident, this scenario is rather hypothetical. It is certain that an exothermic zirconium cladding oxidation in the steam atmosphere would have caused a total loss of the structural integrity of the fuel assemblies for water levels well before a complete drainage could have occurred. Nevertheless, the studies of Boyd [3] indicate that a sufficient cooling of the fuel assemblies due to natural convection in air is possible, providing that the maximum decay heat level per assembly is significantly below 1kW. It is therefore worth studying the thermohydraulic behavior for this particular case and to examine the conditions that must be met in order to ensure enough regions where the flow is in the downward direction. One condition would be a fuel rack design that allows air flow through the fuel assemblies also at water levels above the bottom end of the racks.

Figure 11. Developing Regions with a Downward Flow Direction (green) for a Complete Loss of Coolant. Flow with Upward Tendency Colored in Purple.

Fig. 11 shows the fuel assemblies inside the fuel racks from the top view. The coloring of the fuel assemblies corresponds to the respective volumetric decay heat at a height of 3m from the bottom of the pool floor. The region surrounding the racks is split into two areas. Green depicts the regions of downward flow where air enters between the racks and undercuts along the pool floor. In the purple regions the flow is pointed upward. It can be seen that downward flow occurs only if a very wide space

between the fuel racks exists or at locations where the decay heat level per fuel assembly is significantly below 500W. Air first needs to reach the bottom of the pool. Then it enters the fuel assemblies and eventually cools them accordingly.

5. CONCLUSIONS

The present paper shows how CFD can help to study the safety of spent fuel pools. Important thermohydraulic aspects that require modelling in one-dimensional codes can be addressed directly. One aspect that is so far scarcely studied is the development of the three-dimensional flow- and temperature field in the pool and reactor building atmosphere, given that the fuel assemblies are partially uncovered. It is expected that the spatial arrangement of the fuel racks and the location of the hottest fuel has a strong influence on the cooling of the individual fuel assemblies for the latter scenario. This influence needs to be quantified for different water levels and operating conditions of the building ventilation. Here, the reactor building design that has been in operation at the Fukushima nuclear power plant served as a model case. The simulation results give an insight into the evolving flow paths which were discussed qualitatively. Treating the fuel assemblies as porous bodies appears to be an appropriate modelling approach, reducing the computational effort significantly. A detailed presentation of the emerging cladding temperatures inside the fuel assemblies is not included here, because several local effects such as the heat transfer modelling between the fuel racks still need investigation. Further aspects that need to be examined are the resolution of the computational grid, the turbulence modelling in the pool and building atmosphere, the resulting material properties due to air steam mixing as well as the heat transport phenomena below water which determine the evaporation rates. The authors plan to qualify all these aspects separately, either by means of geometry-resolved calculations or by comparison with test cases from the literature. Quantitative results will be presented in future publications.

ACKNOWLEDGMENTS

The project underlying this report is funded by the German Federal Ministry of Education and Research under the reference number 02NUK027C. The responsibility for the content of this publication lies with the authors. The authors would like to thank the Chair of Hydrogen and Nuclear Energy at the Technical University Dresden (Germany) for supplying experimental data from their ADELA II facility. [8, 9]

SPONSORED BY THE

REFERENCES

1. A. Kaliatka, V. Ognerubov, V. Vileiniškis and E. Ušpuras, “Analysis of the Processes in Spent Fuel Pools in Case of Loss of Heat Removal due to Water Leakage“, *Science and Technology of Nuclear Installations*, **2013**, Article ID 598975 (2013).
2. J. G. Ibarra, W. R. Jones, G. F. Lanik, H. L. Ornstein and S. V. Pullani, “Operating Experience Feedback Report, Assessment of Spent Fuel Cooling”, *U.S. Nuclear Regulatory Commission Report NUREG-1275*, Vol. 12 (1997).
3. C. F. Boyd, “Predictions of Spent Fuel Heatup After a Complete Loss of Spent Fuel Pool Coolant”, *U.S. Nuclear Regulatory Commission Report NUREG-1726*, (2000).

4. A. S. Benjamin, D. J. McCloskey, D. A. Powers and S. A. Dupree, "Spent Fuel Heatup Following Loss of Water During Storage", *U.S. Nuclear Regulatory Commission Report NUREG/CR-0649*, (1979)
5. H. P. Nourbaskhsh, G. Miao and Z. Cheng, "Analysis of Spent Fuel Heatup Following Loss of Water in a Spent Fuel Pool, A User's Manual for the Computer Code SHARP", *U.S. Nuclear Regulatory Commission Report NUREG/CR-6441*, (2002).
6. A. Kaliatka, V. Ognerubov and V. Vileiniskis, "Analysis of the processes in spent fuel pools of Ignalina NPP in case of loss of heat removal", *Nuclear Engineering and Design,* **240**, pp. 1073-1082 (2010).
7. R. Gauntt, D. Kalinich, J. Cardoni, J. Phillips, A. Goldmann, S. Pickering, M. Francis, K. Robb, L. Ott, D. Wang, C. Smith, S. St.Germain, D. Schwieder and C. Phelan, "Fukushima Daiichi Accident Study", *Sandia National Laboratories SAND2012-6173*, (2012)
8. S. Schulz, C. Schuster, A. Hurtado, „Convective heat transfer in a semi-closed BWR-fuel assembly in the absence of water", *Nuclear Engineering and Design,* **272**, pp. 36-44 (2014)
9. S. Schulz, C. Schuster and A. Hurtado, "Experimental Investigation of Boil-Off-Scenario in BWR Spent Fuel Pools" *Proceedings of the 21th International Conference on Nuclear Engineering (ICONE21)*, Chengdu, China, July 29 – August 2, (2013).
10. S. Kakaç, R. K. Shah and W. Aung, *Handbook of single-phase convective heat transfer*, Chapter 7, John Wiley & Sons, Inc., USA/Canada (1987).